SCANNING VOL. 22, 295–303 (2000)


Received: May 15, 2000
Accepted: June 1, 2000

# Field-Emission Scanning Electron Microscopy of the Internal Cellular Organization of Fungi

WALLY H. MÜLLER,*† ADRIAAN C. VAN AELST,‡ BRUNO M. HUMBEL,* THEO P. VAN DER KRIFT,* TEUN BOEKHOUT†

*Department of Molecular Cell Biology, EMSA, Utrecht University, Utrecht; †Yeast Division of the Centraalbureau voor Schimmelcultures, Delft; ‡Department of Experimental Plant Morphology and Cell Biology, Agricultural University of Wageningen, Wageningen, The Netherlands

**Summary:** Internal viewing of the cellular organization of hyphae by scanning electron microscopy is an alternative to observing sectioned fungal material with a transmission electron microscope. To study cytoplasmic organelles in the hyphal cells of fungi by SEM, colonies were chemically fixed with glutaraldehyde and osmium tetroxide and then immersed in dimethyl sulfoxide. Following this procedure, the colonies were frozen and fractured on a liquid nitrogen-precooled metal block. Next, the fractured samples were macerated in diluted osmium tetroxide to remove the cytoplasmic matrix and subsequently dehydrated by freeze substitution in methanol. After critical point drying, mounting, and sputter coating, fractured cells of several basidiomycetes were imaged with field-emission SEM. This procedure produced clear images of elongated and spherical mitochondria, the nucleus, intravacuolar structures, tubular- and plate-like endoplasmic reticulum, and different types of septal pore caps. This method is a powerful approach for studying the intracellular ultrastructure of fungi by SEM.

**Key words:** freeze substitution, fungi, ultrastructure, maceration, scanning electron microscopy

**PACS:** 87.64.Dz, 07.78.+s

## Introduction

Scanning electron microscopy of cellular ultrastructure has been visualized in the pathology, ontogeny, and taxonomy of many organisms. However, most of this work has been performed on animal cells or tissues, such as, for example, blood cells (Haggis 1982, 1992; Nobuo *et al.* 1999), hamster muscle (Patten and Ovalle 1991), and rat liver (Tanaka 1981). Several plant tissues have also been subjected to internal visualization, including the alga *Euglena* (Guttman 1971), chloroplasts (Barnes and Blackmore 1984a, b), and roots (Van Aelst and Wilms 1988; Vesk *et al.* 1994, 1996). By contrast, only a few studies reported on fungal material, such as interactions with host tissues (Brown and Brotzman 1976), formation of arthrospores (Barrera 1983), and septal pore caps in basidiomycetes (Lisker *et al.* 1975; Müller *et al.* 1994, 1995, 1998a, b, 1999).

To image the intracellular ultrastructure of these cells, investigators utilized the following preparation steps: fixation, freezing, fracturing, removing of cytoplasmic material, dehydration, critical point drying, and sputter coating. Chemical fixation of tissues was done by immersion in either buffered glutaraldehyde, or osmium tetroxide, or both. Other than immersion, tissues such as lung and kidney have been successfully fixed by perfusion fixation (Jongebloed and Kalicharan 1994, Tanaka and Mitsushima 1984). In other cases, single cells are embedded in fibrin gels (Haggis and Bond 1978) or in chitosan (Fukudome and Tanaka 1986) prior to fixation. Plant material, such as root tips, was first infiltrated with saponin (Vesk *et al.* 1994). Finally, single cells can be cryofixed (Nobuo *et al.* 1999).

To open up tissues and cells, investigators have employed (1) a tissue sectioner (Brown *et al.* 1976), (2) manually fracturing (El Shennawy *et al.* 1982), (3) oxygen plasma etching (Lee and Nicholls 1983, Richards *et al*. 1993), (4) cryofracturing of tissue embedded in paraffin (Dalen *et al.* 1978), and (5) freeze fracturing (Lea *et al.* 1992). In the latter procedure, the chemically fixed material is first cryoprotected in dimethyl sulfoxide (DMSO), then frozen on a metal plate chilled with liquid nitrogen and fractured with a razor blade and a hammer (Barnes and Blackmore 1984a, 1984b; Haggis 1982; Müller *et al.* 1998a, b; Tanaka 1981). In addition to these methods, monolayers of cells and cell suspensions have been (6) mechanically ruptured (Batten *et al*. 1980, Peters and Carley 1988), (7) thaw-fixed (Haggis 1989), (8) removed by nitrocellulose acetate filter (Beckers *et al*. 1987, Simons and Virta 1987), (9) dry cleaved with Scotch tape (Flood 1975), and (10) wet cleaved (Hohenberg *et al*. 1986).

Address for reprints:

Dr. Wally H. Müller
Dept. Mol. Cell Biology
EMSA, University of Utrecht
Padualaan 8
3584 CH Utrecht, The Netherlands
E-mail: W.H.Muller@bio.uu.nl

After the samples are fractured, the cytoplasmic matrix is removed by rinsing with distilled water (Inoué 1983) or by chemical etching in diluted osmium tetroxide, also known as maceration. The time required to macerate the sample varies with organism. Fukudome and Tanaka (1986) macerated animal cells for 3–5 days, plant or fungal material required three to four times longer (Barnes and Blackmore 1984a, b; Koga *et al.* 1992; Müller *et al.* 1998a, b).

Prior to dehydration, the samples are treated with osmium tetroxide, tannic acid, and osmium tetroxide to enhance electrical conductivity (Barnes and Blackmore 1984b, Kelley *et al.* 1973, Tanaka 1981). Subsequently, the samples are prepared for final imaging of the intracellular ultrastructure.

In the present study we have adapted and modified the maceration methods of Tanaka (1981) and Barnes and Blackmore (1984a,b) in comparative SEM of some filamentous basidiomycetes. With this method we obtained constant quality, and were able to view unprecedented ultrastructural details in hyphae.

## Materials and Methods

### Organisms and Culture Conditions

*Aquathanatephorus pendulus* (CBS 700.82), *Ceratobasidium cornigerum* (CBS 132.82), *Epulorhiza anaticula* (CBS 189.90), *Rhizoctonia solani* AG-3 (CBS 346.84), *Schizophyllum commune* (Monokaryon CBS 340.81, Dikaryon CBS 340.81 × 341.81), and *Trichosporon sporotricoides* (CBS 8245) were maintained on YM agar (YMA, Difco Laboratories, Detroit, Mich., USA). Culture medium was autoclaved for 20 min at about 1.1 bar, 110°C, and aseptically poured into Petri dishes of about 5.3 cm in diameter and 1.5 cm height (Nunclon, Nalge Nunc International, Albertslund, Denmark). After the YMA became solidified, an autoclaved perforated polycarbonate filter (Poretics: Polycarbonate Track Etching (PCTE) filters, Ankersmit, Oosterhout NB, The Netherlands, 0.6 mm pore size and 37 mm filter size) was gently placed on the surface. Cells were scraped from a slant culture and transferred to the PCTE filter. A second autoclaved PCTE filter was placed on top, and the Petri dish was closed. The cells, which were sandwiched between the filters, were allowed to form a colony 2–4 cm in diameter at 24°C.

### Sample Preparation

*Fixation:* Colonies between PCTE-filters in a Petri dish were fixed with 2% (v/v) glutaraldehyde (glutaraldehyde, 70% EM grade, Polysciences, Inc., Warrington, Penna., USA) buffered in 50 mM sodium cacodylate buffer (SCB), pH 7.4. The colonies were fixed for 16 h or longer at 4°C. After fixation, the PCTE filter was removed and the colony was rinsed three times with SCB and three times with 66 mM phosphate buffer (PB), pH 7.4. After rinsing, segments of the colony of about 6 × 15 mm were removed and transferred to a glass screw cap vessel filled with 1% (w/v) osmium tetroxide/ 66 mM PB for 1 h at room temperature (RT) or 16 h at 4°C.

*Cryoprotection:* After postfixation in osmium tetroxide, the fungal material was washed three times with 66 mM PB, and rectangles 4 × 6 mm were removed with a razor blade under 66 mM PB. For orientation purposes, the upper right and the bottom left corner of the rectangle were cut away, and the samples were subsequently immersed in a series of 15, 30, and 50% (v/v) aqueous DMSO for at least 15 min each.

*Freezing and fracturing* (Figs. 1–8): A sample immersed in 50% (v/v) DMSO was placed on Whatman filter to remove excess DMSO (Fig. 2) and then quickly put onto a liquid nitrogen-precooled metal block (Fig. 3). Three samples from the colony were put on the metal block (Fig. 4). Next, the samples were fractured with a liquid nitrogen-precooled razor blade and a hammer (Figs. 5, 6). To prevent the samples from being expelled from the block and lost in the surrounding liquid nitrogen, the block was covered with a glass slide on either side of the knife (Figs. 1, 5, 6; in Figure 7 one glass slide has been removed to show a fractured sample as indicated with an arrow).

*Maceration:* The fractured samples were quickly transferred to a 12-well white porcelain plate (Fig. 8) filled with 50% DMSO in distilled water for about 10 s, and subsequently washed with 66 mM PB. A sketch of each fractured sample was made to document the fractured plane. The fractured fungal samples were macerated in 0.2% osmium tetroxide/ 66 mM PB for 8 to 21 days at RT. About 6 to 10 samples were put in a screw-capped glass vial. After the samples were subjected to maceration, the 0.2% osmium tetroxide in 66 mM PB was changed four times on the first day. Thereafter, one change of fresh 0.2% osmium tetroxide/ 66 mM PB was done each day. The glass vials containing the samples were left undisturbed during maceration at RT.

*Electron conductance:* On a shaker (Swip rotary shaker apparatus, Edmund Bühler, Hechingen, Germany) the vials containing samples were gently agitated at 100 rpm at RT. Next, the samples were subjected to 1 h 1% (w/v) osmium tetroxide/ 66 mM PB, followed by six thorough washings with distilled water to eliminate traces of osmium tetroxide that could react with tannic acid. After washing, the samples were transferred into a clean glass vial filled with 2% (w/v) tannic acid (Lot 1764 KBJA, Mallinckrodt, Inc., Paris, Kentucky, USA) in distilled water for 2 to 16 h at RT. After treatment in tannic acid, the samples were washed several times with distilled water and transferred into a clean glass vial filled with 1% aqueous osmium tetroxide and put on the rotary shaker for 1 h at RT. Then the samples were rinsed with distilled water.

*Cryoprotection:* The samples were subsequently immersed in 15 and 30% (v/v) aqueous N,N-dimethyl-formamide (DMF) (Meissner and Schwarz 1990) for 30 min each on a rotary shaker.

*Plunge freezing:* Each sample was gently put on a copper hood (Bal-Tec, Bu 012 056-T, Balzers, Liechtenstein), and after removal of excess DMF with Whatman filter paper, was manually plunge-frozen in liquid propane, cooled with liquid nitrogen in a KF 80 freezing device (Reichert-Jung, Vienna, Austria). Plastic screw-capped tubes with methanol were placed into an aluminum vial filled with liquid nitrogen in the KF 80 chamber. After solidification of the methanol, four frozen samples were put into each tube that was subsequently capped and stored in liquid nitrogen.

*Freeze substitution:* The frozen samples were transferred under liquid nitrogen to a CS-auto freezing device (Reichert-Jung). After freeze substitution in methanol for at least 16 h at – 85°C, the temperature was gradually raised in steps of 7°C per hour to RT, and the methanol was replaced with acetone-2,2,-dimethoxypropane (DMP) (Merck, Darmstadt, Germany) 1:1, 1:2, 1:3, 1:4, and finally with pure acetone-DMP (1 ml of acidified DMP was added to 100 ml acetone, Dierichs and Dosche 1982, Thorpe and Harvey 1979). The samples were transferred into microporous specimen capsules for critical point drying.

*Critical point drying:* The fungal samples were critical point dried from carbon dioxide according the manufacturer's manual (Bal-Tec, CPD 030).

*Mounting on stubs:* Dried fractured fungal samples were mounted on aluminum stubs with conductive carbon cement (Leit-C, Neubauer, Münster, Germany). The aluminum stubs containing the mounted samples were placed in a Petri dish for at least 16 h at RT to evaporate any excess Leit-C solution.

*Metal coating:* The aluminum stubs with samples were mounted on a transfer holder of the Oxford CT 1500 HF cryopreparation chamber (Oxford Instruments, High Wycombe, UK). Inside the preparation chamber, the samples were coated with platinum by magnetron sputtering for 50 s at $5 \times 10^{-6}$ bar, corresponding to a thickness of about 5 nm.

*Scanning electron microscopy:* The samples were examined in an SEM equipped with a cold field-emission gun

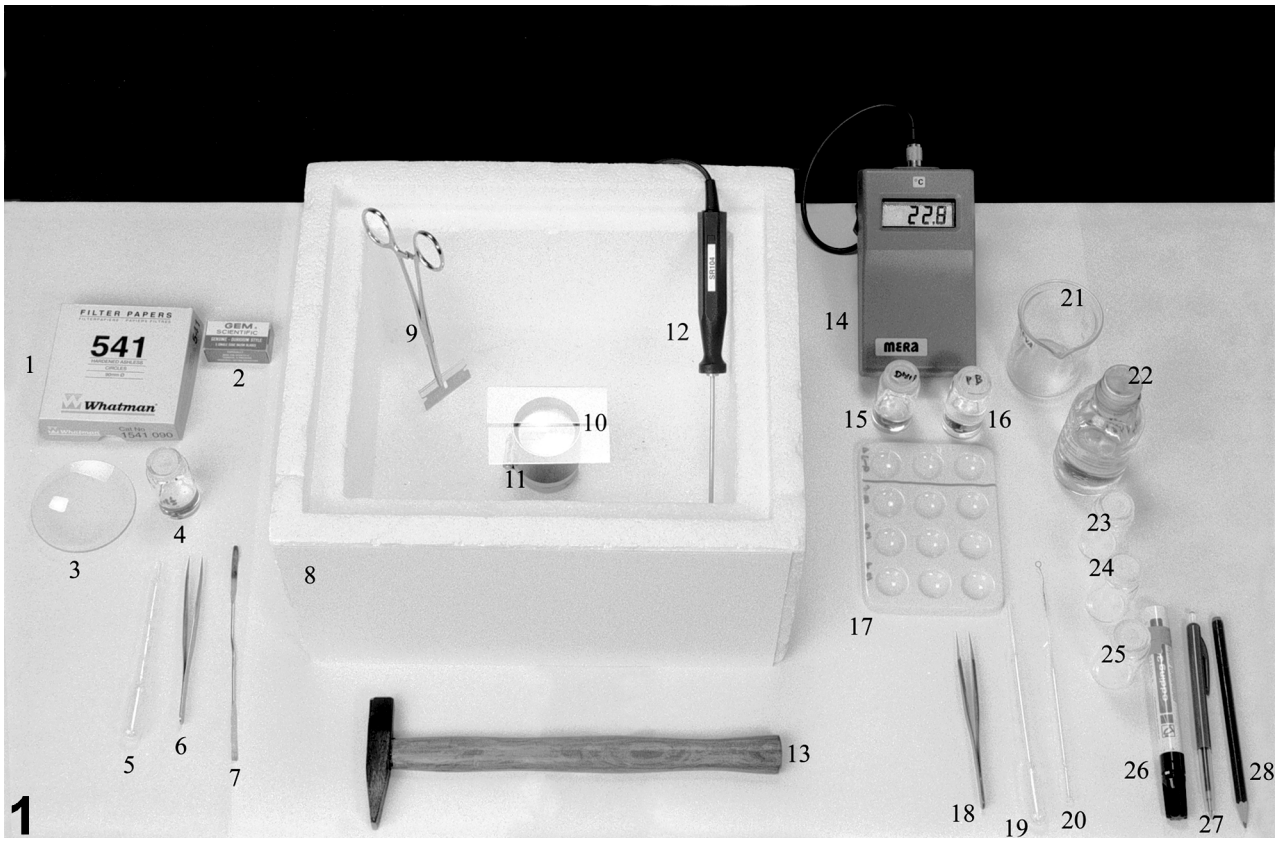


FIG. 1 Materials recommended for freezing and fracturing of fungal samples. 1. Whatman filter paper. 2. Razor blades. 3. Watch-glass to put on the dimethyl sulfoxide (DMSO) infiltrated fungal samples. 4. Samples in vial with 50% DMSO. 5. Plastic pipette to transfer samples from vial onto watch-glass (tip has to be removed if the samples are large). 6. Tweezers. 7. Spatula. 8. Polystyrene foam box (e.g., 26 cm wide, 30 cm long, 17 cm high). 9. Kelly forceps and razor blade. 10. Glass slides. 11. Metal block 4 cm in diameter and 4.5 cm high, with a brass tube around to create a chamber. 12. Temperature meter probe. 13. Small hammer. 14. Temperature meter. 15. Vial containing 50% DMSO. 16. Vial containing phosphate buffer. 17. 12-well white porcelain plate. 18. Tweezers. 19. Plastic pipette to transfer the fractured sample from one well to another. 20. Loop to transfer large fractured samples from one well to another. 21. Beaker to put in waste DMSO and phosphate buffer from the wells. 22. Bottle containing 0.2% osmium tetroxide maceration fluid. 23–25. Vials to put in the fractured samples for maceration. 26–28. Writing materials.

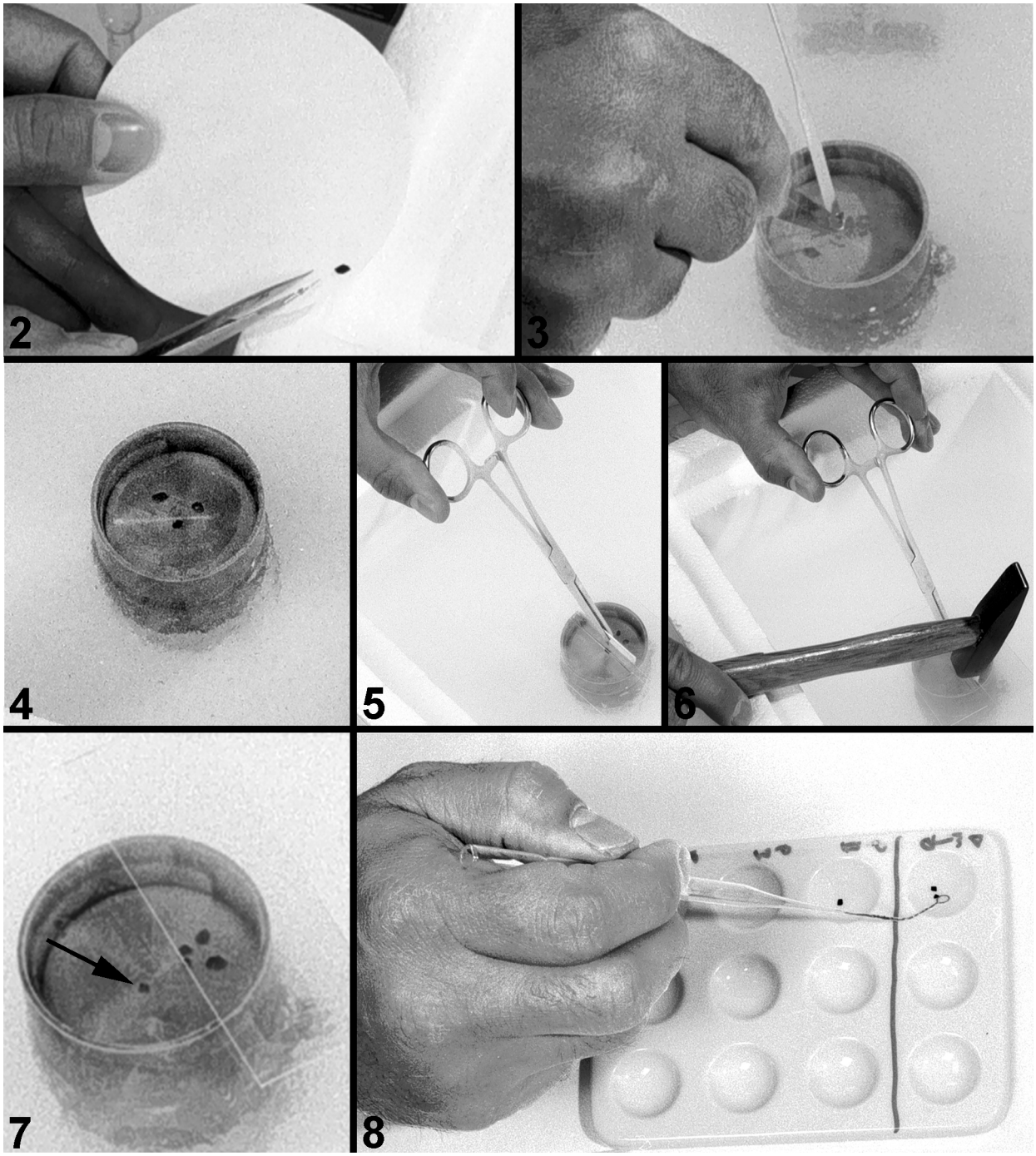


FIG. 2 Before freezing, the excess of dimethyl sulfoxide is removed from the sample by blotting on Whatman filter paper.
FIG. 3 The sample is placed on a cooled metal block with tweezers and a spatula.
FIG. 4 Three frozen samples on the metal block ready to be fractured.
FIG. 5 The razor blade placed on a frozen sample. The metal block is covered with two glass slides.
FIG. 6 Gentle strike of the hammer on the razor blade will fracture the sample.
FIG. 7 Arrow indicates a fragment of a fractured sample. One of the two glass slides has been removed.
FIG. 8 Fractured samples are transferred with tweezers from the metal block to the porcelain plate. The sample is thawed in 50% dimethyl sulfoxide for about 10 s and subsequently transferred with a loop and washed three times with 66 mM phosphate buffer.

(JSM 6300F, JEOL, Peabody, Mass., USA) at an acceleration voltage of 8 kV and a working distance of 6 mm.

## Results

The different types of basidiomycetes required different glutaraldehyde fixation times. Thin hyphae of *Epulorhiza anaticula* or *Cyclomyces fuscus* could easily be fixed for 16 h, but thick hyphae of *Rhizoctonia solani* or *Aquathanatephorus pendulus* required at least 2 days glutaraldehyde fixation. Furthermore, the maceration used in the preparation method appeared to destroy filamentous structures such as cytoskeletal filaments and cytoplasmic protein complexes. However, loss of these structural components resulted in visualization of many of the subcellular organelles including nuclei, endoplasmic reticulum, mitochondria, vacuoles, and septal pore caps (SPCs). For example, the presence of three-dimensional relationships of many of these organelles was readily observed in fractured hyphae of *Trichosporon sporotrichoides* (Fig. 9) and *Schizophyllum commune* (monokaryon) (Fig. 10). Also, at low magnifications the results of fracturing and subsequent maceration in diluted osmium tetroxide could clearly be observed. Unfractured hyphae only revealed their surface of the cell wall. Poorly macerated fungal cells appeared in mostly young hyphae, because the cytoplasm contains more organelles and cytoplasmic structures such as ribosomes as compared with older vacuolated cells. In the colonies, the hyphae growing beneath the surface layer were well fractured and macerated, revealing the spatial relationships of the cell organelles. At high magnification (Fig. 11), the topology of mitochondria, a nucleus, a multi vesicular body, and a vacuole containing tubular structures could be observed in a fractured cell of *T. sporotrichoides*. Tubular endoplasmic reticulum was observed adjacent to the dolipore septum in *Epulorhiza anaticula* (Fig. 12) and *Aquathanatephorus pendulus* (Fig. 13), mitochondria were tubular in *S. commune* (Fig. 10) and *A. pendulus* (Fig. 13), but spherical in *T. sporotrichoides* (Fig. 14) and *E. anaticula* (Fig. 15). Some vacuoles in *T. sporotrichoides* contained an interconnected globular-tubular system that varied in morphology. In Figure 11 the system is more tubular, having lesser globular structures compared with those present in Figure 16. The SPCs varied in size and morphology. The SPCs of *Rhizoctonia solani* (Fig. 17) varied from 1600–2000 nm, having two to five perforations of about 800 nm in diameter. The SPCs of *Ceratobasidium cornigerum* (Fig. 18) varied from 700–900 nm, were about half the size of those SPCs of *R. solani*, and revealed three to five perforations of about 300 nm in diameter. The SPCs of *S. commune* (Fig. 19) varied from 550–650 nm, were about three times smaller than the SPCs of *R. solani*, and revealed about 20 perforations, 60–100 nm in diameter. The imperforate SPCs occurred in *E. anaticula* (Fig. 20) with a pore cap width of about 800 nm.

## Discussion

Imaging the internal ultrastuctural features of fungi with the SEM began in the early 1970s by Laane (1974), who documented the characteristics of vegetative hyphae of *Absidia glauca*. However, the preparation method used did not sufficiently preserve intracellular structures such as mitochondria, vacuoles, and endoplasmic reticulum. Harris *et al.* (1975) clearly showed the internal features of developing perithecia of *Neurospora crassa*. Although their preparation method was successful for imaging perithecia, organelles including the nuclei, vacuoles, mitochondria and endoplasmic reticulum were poorly preserved. Lisker *et al.* (1975) were able to show the perforate septal pore cap in *Rhizoctonia solani*; however, the organelles were not apparent. Brown and Brotzman (1976) clearly showed fungal fructifications, but showed no detailed ultrastructural features. In our study, we adapted and modified the methods of Tanaka (1981) and Barnes and Blackmore (1984a,b). We cultured fungi between filters, prevented loss of fungal samples during fracturing, and implemented freeze substitution of the fungal samples prior to critical point drying.

The preparation method for internal viewing allowed us the visualization of the ultrastructural organization in several different fungi. However, chemical fixation of hyphae may cause ultrastructural changes of organelles and subcellular structures in hyphae from similar structures in living hyphae (Hoch and Howard 1981, Howard and O'Donnell 1987, Müller *et al.* 1991). In basidiomycetes, Hoch and Howard (1981) reported that the SPC and the dolipore septa may be changed in their morphology because of the aldehyde fixation. Müller *et al.* (1991) documented a distortion of the plasma membrane in chemically fixed and freeze-fractured hyphal cells compared with cryofixed and freeze-fractured hyphal cells. Although the combination of cryofixation and freeze substitution may result in better preservation of the subcellular ultrastructure in hyphal cells, many serial sections must be made for final viewing of the topology of their organelles. Alternatively, our method for internal viewing with an SEM clearly showed the morphology of organelles and their spatial relationships. Many hyphal cells can quickly be observed with an SEM, showing not only subcellular ultrastuctural differences in a fungal species, but also revealing differences in ultrastructure between different species. For example, only *Trichosporon sporotrichoides* had an interconnected globular-tubular system in some vacuoles; they were not observed in the other fungal species. At present, this intravacuolar globular-tubular structure has not been characterized.

Cultivation of fungi in medium results in high wet weights. In our initial studies we used this method (Müller *et al.* 1994); however, fracturing the fungi either longitudinally or perpendicularly was difficult, because fungi tended to grow as globules in the liquid medium. Furthermore, fractured cells at the periphery of the globules were difficult to view with the SEM because the fungal hypha

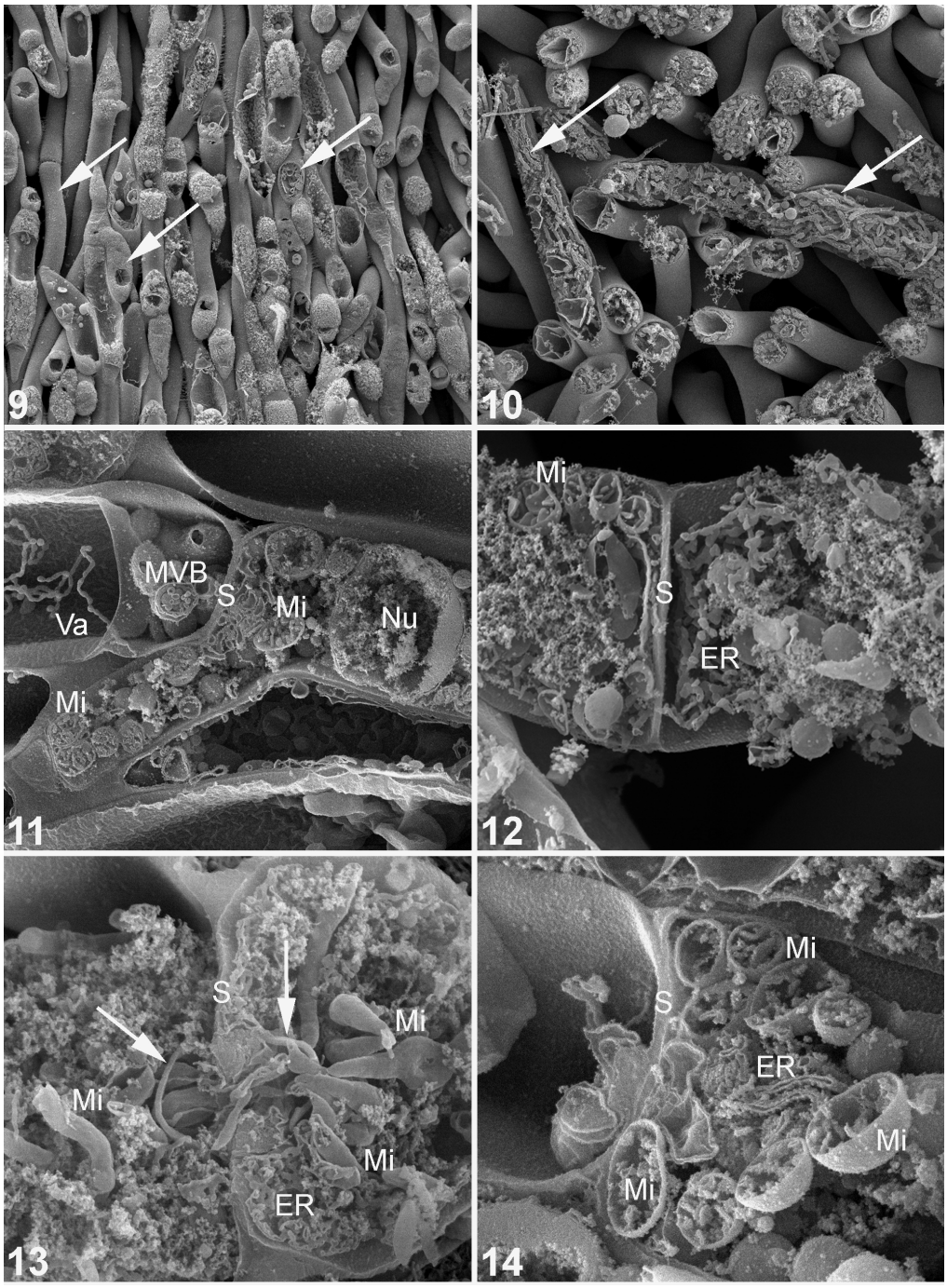


FIG. 9 Scanning electron micrograph of *Trichosporon sporotrichoides* hyphae, which have been fractured. The three arrows from left to right indicate an intact hypha, a poorly macerated hyphal cell, and a sufficiently macerated cell revealing organelles. Horizontal field width = 43.5 µm.
FIG. 10 Scanning electron micrograph of the interior of *Schizopyllum commune* hyphae. The fractured and macerated cells show many tubular-like mitochondria (arrows). Horizontal field width = 28.9 µm.
FIG. 11 A fractured and macerated cell of *Trichosporon sporotrichoides* revealing a nucleus (Nu), globose-ellipsoidal mitochondria (Mi), a multivesicular body (MVB), and a vacuole (Va) containing an interconnected globular-tubular structure. S = septum. Horizontal field width = 10.07 µm.
FIG. 12 Tubular endoplasmic reticulum (ER) flanks the septum (S) in *Epulorhiza anaticula*. Mi = mitochondrion. Horizontal field width = 5.13 µm.
FIG. 13 Mitochondria (Mi) passing through the dolipore septum (S) via the septal pore cap (arrows) in *Aquathanatephorus pendulus*. ER = endoplasmic reticulum. Horizontal field width = 5.13 µm.
FIG. 14 Spherical mitochondria (Mi) are present near the dolipore septum (S) in *Trichosporon sporotrichoides*. ER = endoplasmic reticulum. Horizontal field width = 4.32 µm.

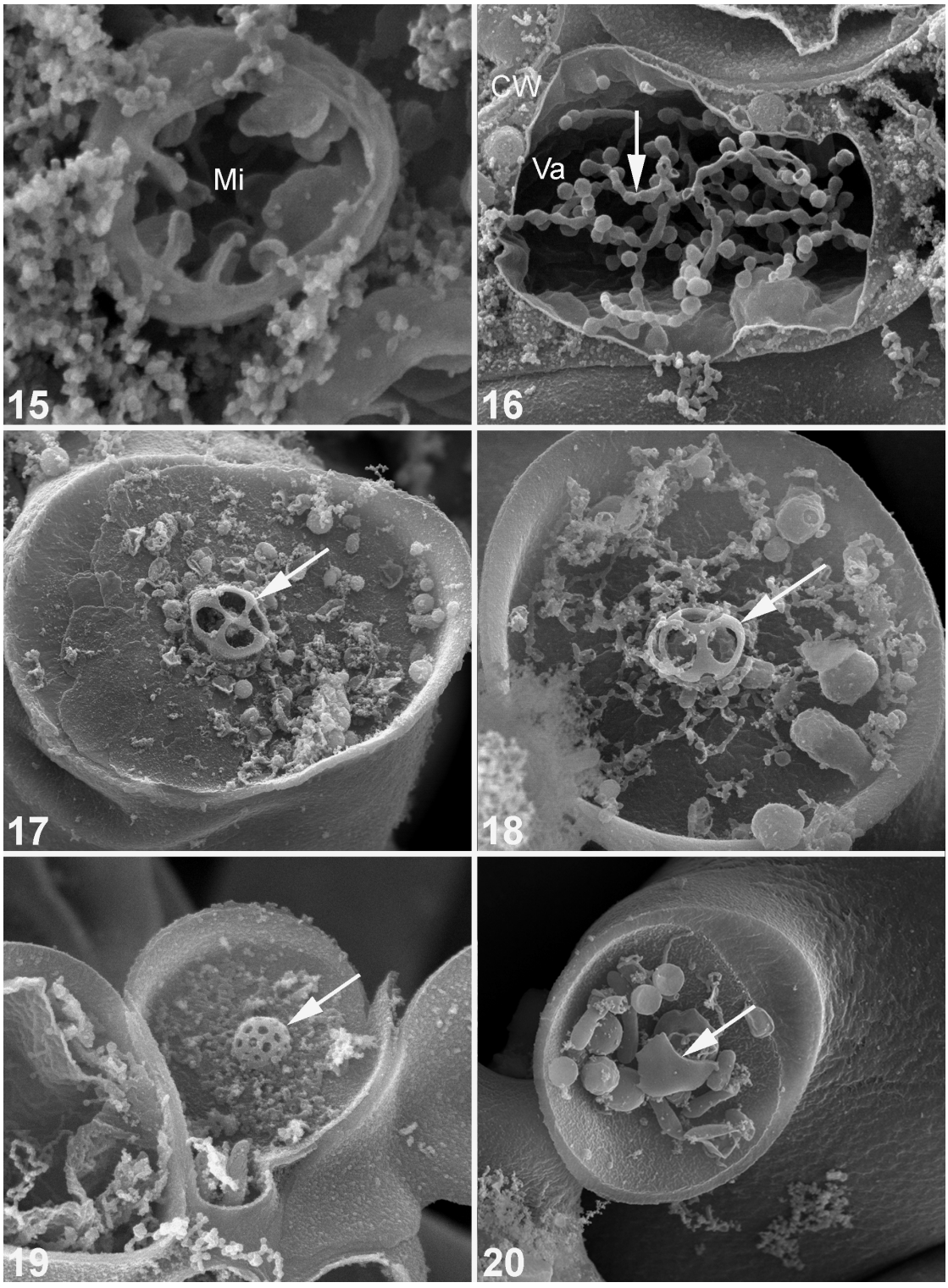


FIG. 15 A spherical mitochondrion (Mi) in *Epulorhiza anaticula* after fracturing and maceration. Note the plate-like cristae. Horizontal field width = 1.04 µm.
FIG. 16 A vacuole (Va) in *Trichosporon sporotrichoides* contains a globular-tubular system that varies in thickness and morphology. CW is the cell wall. Horizontal field width = 4.07 µm.
FIG. 17 The perforate septal pore cap (arrow) of *Rhizoctonia solani* shows four holes. Horizontal field width = 8.33 µm.
FIG. 18 The perforate septal pore cap (arrow) of *Ceratobasidium cornigerum* shows three visible holes. Horizontal field width = 4.94 µm.
FIG. 19 Many small holes are present in the septal pore cap (arrow) of *Schizophyllum commune*. Horizontal field width = 5.57 µm.
FIG. 20 The septal pore cap (arrow) of *Epulorhiza anaticula* is imperforate. Horizontal field width = 6.38 µm.

charged and moved during imaging. These problems were successfully overcome by growing fungi between PCTE filters on agar medium in Petri dishes (Müller *et al.* 1998a, 1998b).

Fixation and postfixation of fungi allowed us to cut the colony into segments for freeze-fracturing. In animal cells, osmium tetroxide is preferred (e.g., Tanaka 1980); glutaraldehyde, which affects the maceration process, is omitted (reviewed by Lea *et al.* 1992). However, when we omitted glutaraldehyde, septal pore caps were not exposed in the fractured samples. Moore and Marchant (1972) suggested that the fracture plane occurs between the plasma membrane and the endoplasmic reticulum near the septum. Perhaps this occurs when either glutaraldehyde was omitted or the endoplasmic reticulum and the septal pore cap were not properly fixed.

To avoid ice crystal damage, different cryoprotectants have been used. Tanaka (1980) and Barnes (1992) included DMSO as a cryoprotectant. However, according to Inoué (1983), DMSO may act not only as a cryoprotectant but also as a dehydration agent and could result in shrinkage of the cells. The reason for the use of DMSO as a cryoprotectant compared with a more volatile one like ethanol (Haggis and Phipps-Todd 1977, Sasaki 1988) is that DMSO, due to its high viscosity, does not evaporate rapidly and the sample is less brittle (A.C. van Aelst, pers. comm.).

Successfully removing the cytoplasmic matrix is critical for imaging internal ultrastuctural features. In animal cells (e.g., Tanaka 1980), this procedure requires a few days of maceration, while for plant cells even longer times are required (Barnes 1992). In our studies, the maceration time required for *R. solani* was about 13 days while that for *S. commune* was only 5 days. Lea *et al.* (1992) suggested that the extraction times are influenced by concentration of the fixative, fixing time, and temperature. The longer the fixation, the longer a maceration time is required. Prolonged maceration with diluted osmium tetroxide will eventually result in both good electrical conductivity and stability of the specimen during observation and image recording.

Most studies employ conventional dehydration in ethanol or acetone. Dehydration in an organic solvent at ambient temperature may cause shrinkage (Boyde 1980); however, this effect can be reduced by the use of t-butyl alcohol (Yu *et al.* 1998). We found that freeze substitution in methanol preserved the fine structure of the cell after maceration more effectively.

Best image condition depends on several factors such as working distance, acceleration voltage, and type of scanning electron microscope. When using the JSM 67300F JEOL scanning electron microscope equipped with a cold field-emission gun, we experimentally found that at a working distance of 6 mm 8 kV acceleration voltage results into best surface information of the specimen, which is the optimal combination of high resolution, low charging, and good contrast.

## Conclusion

Based on our results of imaging the ultrastructure of filamentous basidiomycetes, the preparation method of opening up hyphae is a powerful approach to study the subcellular organization of fungi with an SEM.

## Acknowledgments

The authors thank Dr. D. van der Mei (Centraalbureau voor Schimmelcultures, Baarn, NL) and Dr. W. P. Wergin (Nematology Laboratory, USDA, Beltsville, Md., USA) for critical reading of the manuscript; Professor Dr. A.J. Verkleij (Utrecht University, Utrecht, NL) for fruitful discussion; Wil van Veenendaal, Ronald Leito, Piet Brouwer, and Frits Kindt (Utrecht University, Utrecht, NL) for the preparation of the photographs. This work is based on a cooperative project between the Centraalbureau voor Schimmelcultures, Institute of the Royal Netherlands Academy of Arts and Sciences, and Utrecht University.

## References

Barnes SH: Ultrastructural imaging of freeze-fractured plant cells in the scanning electron microscope. *Microsc Res Techn* 22, 160–169 (1992)

Barnes SH, Blackmore S: Scanning electron microscopy of chloroplast ultrastructure. *Micr Microsc Acta* 15, 187–194 (1984a)

Barnes SH, Blackmore S: Freeze fracture and cytoplasmic maceration in botanical scanning electron microscopy. *J Microsc* 136, RP3–RP4 (1984b)

Barrera CR: Formation and ultrastructure of *Mucor rouxii* arthrospores. *J Bacteriol* 155, 886–895 (1983)

Batten BE, Aaberg JJ, Anderson E: The cytoplasmic filamentous network in cultures ovarian granulosa cells. *Cell* 21, 885–895 (1980)

Beckers CJM, Keller DS, Balch WE: Semi-intact cells permeable to macromolecules: Use in reconstitution for protein transport from the endoplasmic reticulum to the Golgi complex. *Cell* 50, 523–534 (1987)

Boyde A: A review of basic preparation techniques for biological scanning electron microscopy. In *Electron Microscopy*, Vol. 2, *Biology, 1980: Proceedings of the Seventh European Congress on Electron Microscopy, The Hague, The Netherlands, August 24–29, 1980* (Eds. Brederoo P, de Priester W). Seventh European Congress on Electron Microscopy Foundation, Leiden, The Netherlands, 768–777 (1980)

Brown MF, Brotzman HG: Procedures for obtaining sectional views of fungal fruitifications by scanning electron microscopy. *Can J Microbiol* 22, 1252–1257 (1976)

Brown MF, Brotzman HG, Kinden DA: Use of a tissue sectioner to expose internal structures of biological samples for scanning electron microscopy. *Stain Technol* 51, 267–270 (1976)

Dalen H, Myklebust R, Saetersdal TS: Cryofracture of paraffin-embedded heart muscle cells. *J Microsc* 112, 139–151 (1978)

Dierichs R, Dosche C: Problems of the use of 2,2-dimethoxypropane as dehydrating agent in preparing single cells for transmission electron microscopy. *Histochem* 74, 263–269 (1982)

El Shennawy IE, Gee DJ, Aparico SR: A new technique for visualization of internal structure by SEM. *J Microsc* 132, 243–246 (1982)

Flood PR: Dry-fracturing techniques for the study of soft internal biological tissues in the scanning electron microscope. *Scan Electron Microsc* 1975/I,IITRI, Chicago, 287–294 (1975)

Fukudome H, Tanaka K: A method for observing intracellular structures of free cells by scanning electron microscopy. *J Microsc* 141, 171–178 (1986)

Guttman HN: Internal cellular details of *Euglena gracilis* visualized by scanning electron microscopy. *Science* 171, 290–292 (1971)

Haggis GH: Contribution of scanning electron microscopy to reviewing internal cell structure. *Scan Electron Microsc* 2, 751–763 (1982)

Haggis GH: Three-dimensional viewing of internal cell structure. *Scan Electron Microsc* (suppl 3), 179–188 (1989)

Haggis GH: Sample preparation for electron microscopy of internal structure. *Microsc Res Techn* 22, 151–159 (1992)

Haggis GH, Bond EF: Three-dimensional view of the chromatin in freeze-fractured chicken erythrocyte nuclei. *J Microsc* 115, 225–234 (1978)

Haggis GH, Phipps-Tod B: Freeze fracture for electron microscopy. *J Microsc* 111, 193–201 (1977)

Harris JL, Howe HB Jr, Roth IL: Scanning electron microscopy of surface and internal features of developing peritheca of *Neurospora crassa*. *J Bacteriol* 122, 1239–1246 (1975)

Hoch HC, Howard RJ: Conventional chemical fixations induce artifactual swelling of dolipore septa. *Exp Mycol* 5, 167–172 (1981)

Hohenberg H, Bohn W, Rutter G, Mannweiler K: Plasma membrane antigens detected by replica techniques. In *Science of Biological Specimen Preparation* (Eds. Müller M, Becker RP, Boyde A, Wolosewick JJ). SEM Inc., AMF O'Hare, Chicago, (1986) 235–244

Howard RJ, O'Donnell KL: Methodological review: Freeze-substitution of fungi for cytological analysis. *Exp Mycol* 11, 250–269 (1987)

Inoué T: Use of distilled water as a rinsing solution for intracellular observation by scanning electron microscopy. *Scan Electron Microsc* 1, 227–233 (1983)

Jongebloed W, Kalicharan D: Tannic-acid/arginine/osmiumtetroxide fixation of rat tissue by the microwave procedure, observed by SEM. *Beitr Elektronenmikroskop Direktabb Oberfl* 27, 243–252 (1994)

Kelley RO, Dekker RAF, Bluemink JG: Ligand-mediated osmium binding: Its application in coating biological specimens for scanning electron microscopy. *J Ultrastruct Res* 45, 254–258 (1973)

Koga H, Tsukiboshi T, Uematsu T: Application of an osmium-maceration technique to observe plant-microbe interfaces of Italian ryegrass and crown rust fungi by scanning electron microscopy. *Can J Bot* 70, 438–442 (1992)

Laane MM: Scanning electron microscopy of sectioned fungal cells. *Mikroskopie* 30, 163–168 (1974)

Lea PJ, Hollenberg MJ, Temkin RJ, Kahn PA: Chemical extraction of the cytosol using osmium tetroxide for high-resolution scanning electron microscopy. *Microsc Res Techn* 22, 185–193 (1992)

Lee DL, Nicholls CD: The use of plasma etching to reveal the internal structure of *Nippostrongylus brasiliensis* (Nematoda). *Parasitology* 86, 477–480 (1983)

Lisker N, Katan J, Henis Y: Scanning electron microscopy of the septal pore apparatus of *Rhizoctonia solani*. *Can J Bot* 53, 1801–1804 (1975)

Meissner DH, Schwarz H: Improved cryoprotection and freeze-substitution of embryonic quail retina: A TEM study on ultrastructural preservation. *J Electron Microsc Techn* 14, 348–356 (1990)

Moore RT, Marchant R: Ultrastructural characterization of the basidiomycete septum of *Polyporus biennis*. *Can J Bot* 50, 2463–2469 (1972)

Müller WH, Van der Krift TP, Knoll G, Smaal EB, Verkleij AJ: A preparation method of specimens of the fungus *Penicillium chrysogenum* for ultrastructural and immuno-electron microscopical studies. *J Microsc* 169, 29–41 (1991)

Müller W H, Van Aelst AC, Van der Krift TP, Boekhout T: Scanning electron microscopy of the septal pore cap of the basidiomycete *Schizophyllum commune*. *Can J Microbiol* 40, 879–883 (1994)

Müller WH, Van Aelst AC, Van der Krift TP, Boekhout T: Novel approaches to visualize the septal pore cap. *Stud Mycol* 38, 111–117 (1995)

Müller WH, Montijn RC, Humbel BM, Van Aelst AC, Boon EJMC, Van der Krift TP, Boekhout T: Structural differences between two types of basidiomycete septal pore caps. *Microbiology* 144, 1721–1730 (1998a)

Müller WH, Stalpers JA, Van Aelst AC, Van der Krift TP, Boekhout T: Field emission gun-scanning electron microscopy of septal pore caps of selected species in the *Rhizoctonia* s. l. complex. *Mycologia* 90, 170–179 (1998b)

Müller WH, Humbel BM, Van Aelst AC, Van der Krift TP, Boekhout T: The septal pore cap of basidiomycetes. In *Plasmodesmata: Structure, Function, Role in Cell Communication* (Eds. Van Bel A, Van Kesteren P). Springer-Verlag: Berlin, Germany (1999) 119–127

Nobuo T, Yasuhisa F, Hideho U, Yasuko K, Takeshi B, Ryoichi H, Shinichi O: Ultrastructural changes of erythrocyte membrane skeletons in chorea-acanthocytosis and McLeod syndrome revealed by the quick-freezing and deep-etching method. *Acta Haematol* 101, 25–31 (1999)

Patten RM, Ovalle WK: Muscle spindle ultrastructure revealed by conventional and high-resolution scanning electron microscopy. *Anat Rec* 230, 183–198 (1991)

Peters K-R, Carley WM: Attachment of plasma membranes of cultures cells to silicon chips for high magnification imaging in scanning electron microscopy. *Scan Microsc* 2, 2055–2066 (1988)

Richards RG, Lloyd PC, Rahn BA, Gwynn IA: A new method for investigating the undersurface of cell monolayers by scanning electron microscopy. *J Microsc* 171, 205–213 (1993)

Sasaki K: A simple method to observe intracellular organelles with the scanning electron microscope. *J Electron Microsc* 37, 171–173 (1988)

Simons K, Virta H: Perforated MDCK cells support intracellular transport. *EMBO J* 6, 2241–2247 (1987)

Tanaka K: Scanning electron microscopy of intracellular structures. *Int Rev Cytol* 68, 97–125 (1980)

Tanaka K: Demonstration of intracellular structures by high resolution scanning electron microscopy. *Scan Electron Microsc* 1981/II, SEM Inc., AMF O'Hare, Chicago (1981) 1–8

Tanaka K, Mitsushima A: A preparation method for observing intracellular structures by scanning electron microscopy. *J Microsc* 133, 213–222 (1984)

Thorpe JR, Harvey DM: Optimizing and investigation of the use of 2,2-dimethoxypropane as a dehydrating agent for plant tissues in transmission electron microscopy. *J Ultrastruct Res* 68, 186–194 (1979)

Van Aelst AC, Wilms HJ: A scanning electron microscopic method for intracellular and extracellular structure. *Stain Technol* 63, 327–328 (1988)

Vesk PA, Rayns DG, Vesk M: Imaging plant microtubules with high resolution scanning electron microscopy. *Protoplasma* 182, 71–74 (1994)

Vesk PA, Vesk M, Gunning BES: Field emission scanning electron microscopy of microtubule arrays in higher plants. *Protoplasma* 195, 168–182 (1996)

Yu Y, Leng CG, Terada N, Ohno S: Scanning electron microscopic study of the renal glomerulus by an in vivo cryotechnique combined with freeze-substitution. *J Anat* 192, 595–603 (1998)